

Article

New Antioxidant Caffeate Esters of Fatty Alcohols Identified in *Robinia pseudoacacia*

Ágnes M. Móricz ^{1,*} , Márton Baglyas ^{1,2} , András Darcsi ³ , József Balla ⁴ and Gertrud E. Morlock ⁵ 

¹ Plant Protection Institute, HUN-REN Centre for Agricultural Research, Fehérvári út 132–144, 1116 Budapest, Hungary; baglyas.marton@atk.hun-ren.hu

² Doctoral School, Semmelweis University, Üllői út 26, 1085 Budapest, Hungary

³ Pharmaceutical Chemistry and Technology Department, National Center for Public Health and Pharmacy, Szabolcs utca 33, 1135 Budapest, Hungary; darcsi.andrew@gmail.com

⁴ Department of Inorganic and Analytical Chemistry, Faculty of Chemical Technology and Biotechnology, Budapest University of Technology and Economics, Szent Gellért tér 4, 1111 Budapest, Hungary; balla.jozsef@vbk.bme.hu

⁵ Institute of Nutritional Science, Chair of Food Science, Justus Liebig University Giessen, Heinrich-Buff-Ring 26–32, 35392 Giessen, Germany; gertrud.morlock@uni-giessen.de

* Correspondence: moricz.agnes@atk.hun-ren.hu

Abstract: The stem bark of black locust (*Robinia pseudoacacia* L.) was extracted, and nine antioxidant compounds (**R1–R9**) were detected by high-performance thin-layer chromatography combined with the radical scavenging 2,2-diphenyl-1-picrylhydrazyl (DPPH•) assay, multi-detection, and heated electrospray high-resolution mass spectrometry. For structure elucidation, the methanolic crude extract was fractionated by solid-phase extraction, and the compounds were isolated by reversed-phase high-performance liquid chromatography with diode array detection. The structures of isolated compounds were elucidated by nuclear magnetic resonance and attenuated total reflectance Fourier-transform infrared spectroscopy as well as gas chromatography-mass spectrometry to determine the double bond position. 3-*O*-Caffeoyl oleanolic acid (**R1**), oleyl (**R2**), octadecyl (**R3**), gadoleyl (**R4**), eicosanyl (**R5**), (*Z*)-9-docosenyl (**R6**), docosyl (**R7**), tetracosyl (**R8**), and hexacosanyl (**R9**) caffeates were identified. While **R1** has been reported in *R. pseudoacacia* stem bark, the known **R3**, **R5**, **R7**, **R8**, and **R9** are described for the first time in this species, and the **R2**, **R4**, and **R6** are new natural compounds. All nine caffeates demonstrated antioxidant activity. The antioxidant effects of the isolated compounds **R1–R8** were quantified by a microplate DPPH• assay, with values ranging from 0.29 to 1.20 mol of caffeic acid equivalents per mole of isolate.

Keywords: black locust (*Robinia pseudoacacia* L.); phenolic esters of fatty alcohols; high-performance thin-layer chromatography—effect-directed analysis (HPTLC-EDA); antioxidant assay; heated electrospray high-resolution mass spectrometry (HESI-HRMS); bioassay-guided isolation; solid-phase extraction (SPE); reversed-phase high-performance liquid chromatography with diode array detection (RP-HPLC-DAD); nuclear magnetic resonance (NMR) spectroscopy; attenuated total reflectance Fourier-transform infrared (ATR-FTIR) spectroscopy; gas chromatography-mass spectrometry (GC-MS)



Citation: Móricz, Á.M.; Baglyas, M.; Darcsi, A.; Balla, J.; Morlock, G.E. New Antioxidant Caffeate Esters of Fatty Alcohols Identified in *Robinia pseudoacacia*. *Molecules* **2024**, *29*, 5673. <https://doi.org/10.3390/molecules29235673>

Academic Editors: Simona Fabroni, Krystian Marszałek and Aldo Todaro

Received: 25 October 2024

Revised: 25 November 2024

Accepted: 28 November 2024

Published: 30 November 2024



Copyright: © 2024 by the authors. Licensee MDPI, Basel, Switzerland. This article is an open access article distributed under the terms and conditions of the Creative Commons Attribution (CC BY) license (<https://creativecommons.org/licenses/by/4.0/>).

1. Introduction

The North American black locust (*Robinia pseudoacacia* L., family Fabaceae) has been widely planted all over the world, initially as an ornamental tree and later for soil and water conservation, like in Europe since the 17th century [1,2]. It is a fast-growing tree that reproduces both sexually and vegetatively; therefore, it has become one of the most aggressively invasive woody plants with a high biomass worldwide [2]. Due to its allelopathic potential, it often overgrows the indigenous plants, and as a nitrogen-fixing species, it can alter the native vegetation [3]. Despite its environmental drawbacks, it offers

economic benefits, particularly in the honey and wood industries [4]. Furthermore, black locust has been used in traditional folk medicine, especially in Europe and Asia, due to its astringent, cholagogue, diuretic, anti-inflammatory, purgative, spasmolytic, and sedative properties, as well as Cherokee treated toothache with it [5,6]. Its beneficial effects [7,8], such as antibacterial, antifungal, antioxidant, anti-inflammatory, and cytotoxic properties, are primarily attributed to the high content of diverse phenoloids [9]. Flowers and leaves are rich sources of phenolic acids (e.g., caffeoylquinic acids, caffeic and coumaric acids and their hexosides, coumaroylquinic acids, ellagic acid hexoside, gallic acid, and *p*-hydroxybenzoic acid), flavonoids (apigenin, catechin, procyanidin dimers and trimers, quercetin and kaempferol derivatives, and vescalagins), and tannins [9,10], all of which exhibit various biological activities. The diversity of flavonoid aglycones and hydroxycinnamic acid derivatives originated from propolis and nectar-derived kaempferol glycosides enables the floral authentication of black locust honey [11]. However, black locust also contains toxic glycoproteins, lectins, and the homo-monoterpene robinlin that can possess pharmacological activities beyond cytotoxicity [12].

The wood of *R. pseudoacacia* is predominantly composed of structural polysaccharides (e.g., cellulose, hemicellulose, and lignin) that conceal a wide range of valuable compounds [13], and it can be the source of biofuels [14]. The heartwood contains several phenolic acids (e.g., caffeic acid, chlorogenic acid, ellagic acid, ferulic acid, *p*-coumaric acid, gallic acid, ellagic acid, *p*-hydroxybenzoic acid, and protocatechuic acid), flavonoids (e.g., di-*O*-methylquercetin B, quercetin, epigallocatechin, fustin, catechin, kaempferol, myricetin, procyanidin dimer, robinetin, and dihydrorobinetin), along with stilbenes (resveratrol and piceatannol) [15–17]. Interestingly, the bark lacks robinetin, but dihydrorobinetin and phenolic acids like catechin, epicatechin, caffeic acid, and ferulic acid have been detected as defensive compounds in the bark [18,19].

Plant phenolics play a pivotal role in plant growth, development, and defense by displaying antioxidant, antimicrobial, allelopathic, and UV-blocking effects [20]. Reactive oxygen species (ROS) and free radicals are essential for cell signaling and other vital physiological processes. However, during various diseases, including inflammatory and infectious conditions, their overproduction can lead to potential cellular damage [20–22]. Natural antioxidants, such as phenolic compounds, can diminish this unfavorable effect by scavenging the free radicals and converting them into stable forms [23]. High-performance thin-layer chromatography combined with multi-detection (HPTLC–UV/VIS/FLD), the 2,2-diphenyl-1-picrylhydrazyl (DPPH•) assay, and derivatization via the Natural Product reagent A ensure an efficient, high-throughput screening for identifying antioxidant compounds in complex matrices, such as plant extracts [24–26]. It is an effective monitoring tool in bioactivity-guided compound isolation [27].

The study aimed at screening, characterization, isolation, and identification of antioxidant compounds from the methanolic bark extracts of the black locust. Various analytical techniques were utilized, including reversed-phase (RP)-HPTLC–DPPH• assay, RP-HPTLC–UV/VIS/FLD–densitometry, RP-HPTLC–heated electrospray high-resolution mass spectrometry (HESI–HRMS), reversed-phase high-performance liquid chromatography diode array detection (RP–HPLC–DAD), attenuated total reflectance Fourier-transform infrared (ATR–FTIR) spectroscopy, nuclear magnetic resonance (NMR) spectroscopy, and gas chromatography–mass spectrometry (GC–MS). The antioxidant activity of the isolated compounds was assessed by a DPPH• microplate assay.

2. Results and Discussion

2.1. RP-HPTLC–DPPH• Assay Screening and Assignment by RP-HPTLC–HESI–HRMS

Antioxidant compounds of the methanolic crude extract obtained from the black locust bark were separated on RP18 HPTLC plates using acetonitrile—ethanol 3:2 *V/V* as a mobile phase and detected via fluorescence detection (FLD) after derivatization with the Natural Product reagent A and via white light illumination (Vis) after the radical scavenging DPPH• assay (Figure 1d–g). Nine antioxidant compound zones at hR_F 16 (**R9**), 22 (**R8**), 28 (**R7**), 33

(R5), 37 (R6), 42 (R3), 46 (R4), 54 (R2), and 68 (R1) were revealed. Via the derivatization with the Natural Product reagent A, the natively weak blue fluorescence of the zones R1–R9 was enhanced, indicating that the compounds responsible for the antioxidant effect belong to the group of phenolics.

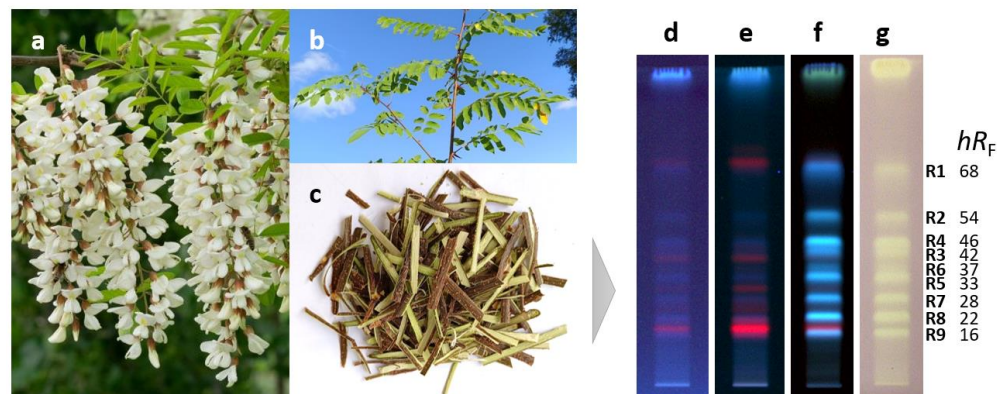


Figure 1. Flowers (a), stem with leaves (b), and stem bark (c) of *Robinia pseudoacacia* along with HPTLC chromatograms of bark crude extract (3 μ L) separated on RP18 plates with acetonitrile-ethanol 3:2 V/V and detected at 254 nm (d), 365 nm (e), and after derivatization with natural product reagent A at 365 nm (f) as well as after the DPPH• assay under white light illumination (g) revealing the antioxidant compounds R1–R9.

This hypothesis (regarding the presence of phenolics) was confirmed by their densitometrically recorded RP-HPTLC–UV spectra showing characteristic absorption bands between 300 and 350 nm (Figure S1). The antioxidant compounds were further characterized by RP-HPTLC–HESI–HRMS. In the positive ionization mode, the intensity of signals corresponding to sodium adducts ($[M+Na]^+$) was low, whereas in the negative ionization mode, signals of deprotonated molecules ($[M-H]^-$) were intense (Table 1).

Table 1. Antioxidant compounds (R1–R9) isolated from the bark extract of black locust detected by RP-HPTLC–DPPH•–Vis and characterized by RP-HPTLC–HRMS.

Isolates	hR_F	Observed m/z [M–H] [−]	Theoretical m/z [M–H] [−]	Error (ppm)	Proposed Molecular Formula	Isolated Amount (mg)	Assignment
R1	68	617.3848	617.3848	0.1	C ₃₉ H ₅₄ O ₆	2.1	3-O-caffeoyl oleanolic acid
R2	54	429.3005	429.3010	−1.2	C ₂₇ H ₄₂ O ₄	1.3	oleyl caffeate
R3	46	431.3162	431.3167	−1.2	C ₂₇ H ₄₄ O ₄	2.3	octadecyl caffeate
R4	42	457.3318	457.3323	−1.1	C ₂₉ H ₄₆ O ₄	2.0	gadoleyl caffeate
R5	33	459.3475	459.3480	−1.1	C ₂₉ H ₄₈ O ₄	1.7	eicosanyl caffeate
R6	37	485.3631	485.3636	−1.0	C ₃₁ H ₅₀ O ₄	0.6	(Z)-9-docosenyl caffeate
R7	28	487.3788	487.3793	−1.0	C ₃₁ H ₅₂ O ₄	1.4	docosyl caffeate
R8	22	515.4101	515.4106	−1.0	C ₃₃ H ₅₆ O ₄	0.9	tetracosyl caffeate
R9	16	543.4414	543.4419	−0.9	C ₃₅ H ₆₀ O ₄	0.9	hexacosanyl caffeate

2.2. Fractionation by Solid-Phase Extraction and Isolation by RP-HPLC–DAD

The methanolic crude extract was fractionated by reversed-phase solid-phase extraction (SPE). The separation and peak identification of the compounds were achieved by RP-HPLC–DAD–ESI–MS. The isolation from the ethanol eluate was carried out by

RP-HPLC–DAD (Figure 2). The yields of compounds **R1–R9** ranged from 0.9 to 2.3 mg (Table 1), which were used for subsequent structure elucidation.

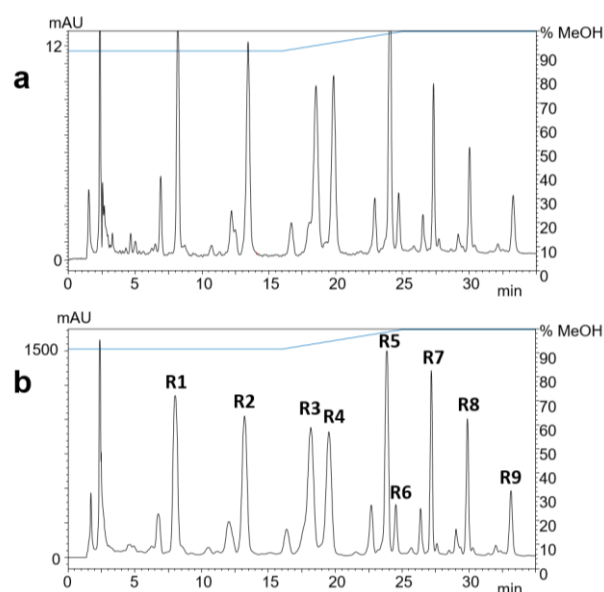


Figure 2. RP-HPLC-UV chromatograms at 323 nm of 1 μ L (a) and 100 μ L (b) of black locust bark extract after SPE. Compounds **R1–R9** were identified by ESI-MS.

2.3. Results of NMR and ATR-FTIR Spectra Recording

The NMR (Figures S3–S35) and ATR-FTIR spectra (Figures S36–S41) were recorded, and the data were compiled and listed as follows for 3-*O*-caffeoyl oleanolic acid (**R1**): IR (ATR) ν_{\max} 3191, 2941, 2927, 2854, 1696, 1600, 1524, 1463, 1389, 1365, 1266, 1170, 1146, 1117, 1019 cm^{-1} ; ^1H and ^{13}C NMR data (Table 2).

Table 2. ^1H and ^{13}C NMR (CD_3OD , 600/151 MHz) resonance assignments of 3-*O*-caffeoyl oleanolic acid (**R1**).

Position	δ_{H} (J in Hz)	δ_{C} , Type
1a	1.69 (m, 1H)	39.4, CH_2
1b	1.10 (m, 1H)	
2a	1.72 (m, 1H)	24.7, CH_2
2b	1.67 (m, 1H)	
3	4.57 (dd, $J = 11.5, 4.3$ Hz, 1H)	82.3, CH
4	-	39.0, C
5	0.91 (m, 1H)	56.8, CH
6a	1.59 (m, 1H)	19.4, CH_2
6b	1.47 (m, 1H)	
7a	1.56 (m, 1H)	33.9, CH_2
7b	1.34 (m, 1H)	
8	-	40.6, C
9	1.66 (m, 1H)	49.1, CH
10	-	38.2, C
11	1.92 (m, 2H)	24.5, CH_2
12	5.26 (t, $J = 3.6$ Hz, 1H)	123.5, CH

Table 2. Cont.

Position	δ_H (J in Hz)	δ_C , Type
13	-	145.3, C
14	-	42.9, C
15a	1.79 (m, 1H)	28.9, CH ₂
15b	1.09 (m, 1H)	
16a	2.02 (td, $J = 13.5, 3.5$ Hz, 1H)	24.1, CH ₂
16b	1.60 (m, 1H)	
17	-	47.7, C
18	2.86 (dd, $J = 13.9, 4.6$ Hz, 1H)	42.8, CH
19a	1.70 (m, 1H)	47.3, CH ₂
19b	1.14 (m, 1H)	
20	-	31.6, C
21a	1.40 (td, $J = 13.8, 3.8$ Hz, 1H)	34.9, CH ₂
21b	1.20 (m, 1H)	
22a	1.77 (m, 1H)	33.9, CH ₂
22b	1.55 (m, 1H)	
23	0.91 (s, 3H)	28.7, CH ₃
24	0.97 (s, 3H)	17.3, CH ₃
25	1.01 (s, 3H)	15.9, CH ₃
26	0.84 (s, 3H)	17.7, CH ₃
27	1.19 (s, 3H)	26.4, CH ₃
28	-	182.1, C
29	0.91 (s, 3H)	33.6, CH ₃
30	0.95 (s, 3H)	24.0, CH ₃
1'	7.03 (d, $J = 2.0$ Hz, 1H)	115.1, CH
2'	-	146.7, C
3'	-	149.6, C
4'	6.78 (d, $J = 8.2$ Hz, 1H)	116.5, CH
5'	6.94 (dd, $J = 8.2, 2.1$ Hz, 1H)	122.9, CH
6'	-	127.8, C
7'	7.52 (d, $J = 15.8$ Hz, 1H)	146.7, CH
8'	6.24 (d, $J = 15.9$ Hz, 1H)	115.6, CH
9'	-	169.2, C

Oleyl caffeate (**R2**): IR (ATR) ν_{\max} 2924, 2854, 1712, 1593, 1509, 1460, 1370, 1263, 1167, 1121, 1091, 1050, 1018 cm^{-1} ; ^1H NMR (CD_3OD , 600 MHz) δ 7.53 (d, $J = 16.0$ Hz, 1H, H-7'), 7.04 (d, $J = 2.1$ Hz, 1H, H-1'), 6.94 (dd, $J = 8.3, 2.1$ Hz, 1H, H-5'), 6.78 (d, $J = 8.1$ Hz, 1H, H-4'), 6.25 (d, $J = 15.9$ Hz, 1H, H-8'), 5.34 (m, 2H, H-9, H-10), 4.17 (t, $J = 6.6$ Hz, 2H, H-1), 2.03 (m, 4H, H-8, H-11), 1.69 (p, $J = 7.0$ Hz, 2H, H-2), 1.41 (m, 2H, H-3), 1.29 (br s, 20H, H-4–H-7, H-12–H-17), 0.91 (m, 3H, H-18); ^{13}C NMR (CD_3OD , 151 MHz) δ (2D HSQC, HMBC) 169.5 (C, C-9'), 149.7 (C, C-3'), 146.9 (C, C-2'), 146.8 (CH, C-7'), 130.8 (CH, C-9), 130.8 (CH, C-10), 127.8 (C, C-6'), 122.9 (CH, C-5'), 116.6 (CH, C-4'), 115.3 (CH, C-8'), 115.1 (CH, C-1'), 65.6 (CH₂, C-1), 33.2 (CH₂, C-16), 30.9–30.2 (CH₂, C-4–C-7, C-12–C-15), 29.8 (CH₂, C-2), 28.0 (CH₂, C-8, C-11), 27.1 (CH₂, C-3), 23.4 (CH₂, C-17), 14.4 (CH₃, C-18)

Octadecyl caffeate (**R3**): IR (ATR) ν_{\max} 3222, 2918, 2851, 1710, 1593, 1520, 1466, 1382, 1269, 1165, 1119, 1077, 1049 cm^{-1} ; ^1H NMR (CD_3OD , 600 MHz) δ 7.53 (d, $J = 15.9$ Hz, 1H, H-7'), 7.04 (d, $J = 2.1$ Hz, 1H, H-1'), 6.94 (dd, $J = 8.1, 2.1$ Hz, 1H, H-5'), 6.78 (d, $J = 8.2$ Hz, 1H, H-4'), 6.25 (d, $J = 15.9$ Hz, 1H, H-8'), 4.17 (t, $J = 6.6$ Hz, 2H, H-1), 1.70 (p, $J = 6.8$ Hz, 2H, H-2), 1.41 (m, 2H, H-3), 1.29 (br s, 28H, H-4–H-17), 0.90 (t, $J = 7.0$ Hz, 3H, H-18); ^{13}C NMR (CD_3OD , 151 MHz) δ 169.4 (C, C-9'), 149.6 (C, C-3'), 146.8 (C, C-2'), 146.8 (CH, C-7'), 127.7 (C, C-6'), 122.9 (CH, C-5'), 116.5 (CH, C-4'), 115.2 (CH, C-8'), 115.1 (CH, C-1'), 65.6 (CH_2 , C-1), 33.1 (CH_2 , C-16), 30.8–30.6 (CH_2 , C-6–C-15), 30.5 (CH_2 , C-4), 30.3 (CH_2 , C-5), 29.8 (CH_2 , C-2), 27.1 (CH_2 , C-3), 23.7 (CH_2 , C-17), 14.4 (CH_3 , C-18)

Gadoleyl caffeate (**R4**): IR (ATR) ν_{\max} 2925, 2854, 1713, 1683, 1648, 1592, 1540, 1459, 1347, 1266, 1165, 1122, 1050, 1013 cm^{-1} ; ^1H NMR (CD_3OD , 600 MHz) δ 7.53 (d, $J = 16.0$ Hz, 1H, H-7'), 7.04 (d, $J = 2.1$ Hz, 1H, H-1'), 6.94 (dd, $J = 8.1, 2.0$ Hz, 1H, H-5'), 6.78 (d, $J = 8.1$ Hz, 1H, H-4'), 6.25 (d, $J = 15.9$ Hz, 1H, H-8'), 5.34 (m, 2H, H-9, H-10), 4.17 (t, $J = 6.6$ Hz, 2H, H-1), 2.03 (m, 4H, H-8, H-11), 1.69 (p, $J = 7.1$ Hz, 2H, H-2), 1.41 (m, 2H, H-3), 1.29 (br s, 24H, H-4–H-7, H-12–H-19), 0.91 (m, 3H, H-20); ^{13}C NMR (CD_3OD , 151 MHz) δ (2D HSQC, HMBC) 169.5 (C, C-9'), 149.6 (C, C-3'), 146.9 (C, C-2'), 146.8 (CH, C-7'), 130.8 (CH, C-9), 130.8 (CH, C-10), 127.8 (C, C-6'), 123.0 (CH, C-5'), 116.6 (CH, C-4'), 115.3 (CH, C-8'), 115.1 (CH, C-1'), 65.6 (CH_2 , C-1), 33.1 (CH_2 , C-18), 30.9–30.2 (CH_2 , C-4–C-7, C-12–C-17), 29.8 (CH_2 , C-2), 28.0 (CH_2 , C-8, C-11), 27.1 (CH_2 , C-3), 23.4 (CH_2 , C-19), 14.4 (CH_3 , C-20)

Eicosanyl caffeate (**R5**): IR (ATR) ν_{\max} 3327, 2918, 2851, 1713, 1599, 1523, 1468, 1380, 1265, 1165, 1118, 1089, 1048 cm^{-1} ; ^1H NMR (CD_3OD , 600 MHz) δ 7.53 (d, $J = 15.9$ Hz, 1H, H-7'), 7.04 (d, $J = 2.0$ Hz, 1H, H-1'), 6.94 (dd, $J = 8.3, 2.1$ Hz, 1H, H-5'), 6.78 (d, $J = 8.2$ Hz, 1H, H-4'), 6.25 (d, $J = 15.9$ Hz, 1H, H-8'), 4.17 (t, $J = 6.6$ Hz, 2H, H-1), 1.70 (p, $J = 6.9$ Hz, 2H, H-2), 1.41 (m, 2H, H-3), 1.29 (br s, 32H, H-4–H-19), 0.90 (t, $J = 7.0$ Hz, 3H, H-20); ^{13}C NMR (CD_3OD , 151 MHz) δ (2D HSQC, HMBC) 169.5 (C, C-9'), 149.7 (C, C-3'), 146.9 (C, C-2'), 146.8 (CH, C-7'), 127.8 (C, C-6'), 122.9 (CH, C-5'), 116.5 (CH, C-4'), 115.2 (CH, C-8'), 115.1 (CH, C-1'), 65.6 (CH_2 , C-1), 33.1 (CH_2 , C-18), 30.8–30.0 (CH_2 , C-4–C-17), 29.8 (CH_2 , C-2), 27.1 (CH_2 , C-3), 23.7 (CH_2 , C-19), 14.4 (CH_3 , C-20)

(*Z*)-9-docosenyl caffeate (**R6**): ^1H NMR (CD_3OD , 600 MHz) δ 7.53 (d, $J = 16.0$ Hz, 1H, H-7'), 7.04 (d, $J = 2.0$ Hz, 1H, H-1'), 6.94 (dd, $J = 8.0, 1.7$ Hz, 1H, H-5'), 6.78 (d, $J = 8.1$ Hz, 1H, H-4'), 6.25 (d, $J = 15.9$ Hz, 1H, H-8'), 5.34 (m, 2H, H-9, H-10), 4.17 (t, $J = 6.5$ Hz, 2H, H-1), 2.03 (m, 4H, H-8, H-11), 1.70 (m, 2H, H-2), 1.41 (m, 2H, H-3), 1.29 (br s, 28H, H-4–H-7, H-12–H-21), 0.90 (t, $J = 6.7$ Hz, 3H, H-22)

Docosyl caffeate (**R7**): IR (ATR) ν_{\max} 2917, 2850, 1716, 1583, 1512, 1467, 1433, 1373, 1259, 1168, 1120, 1056 cm^{-1} ; ^1H NMR (CD_3OD , 600 MHz) δ 7.53 (d, $J = 15.9$ Hz, 1H, H-7'), 7.04 (d, $J = 2.1$ Hz, 1H, H-1'), 6.94 (dd, $J = 8.2, 2.1$ Hz, 1H, H-5'), 6.78 (d, $J = 8.2$ Hz, 1H, H-4'), 6.25 (d, $J = 15.8$ Hz, 1H, H-8'), 4.17 (t, $J = 6.6$ Hz, 2H, H-1), 1.70 (p, $J = 6.8$ Hz, 2H, H-2), 1.40 (m, 2H, H-3), 1.29 (br s, 36H, H-4–H-21), 0.90 (t, $J = 7.1$ Hz, 3H, H-22); ^{13}C NMR (CD_3OD , 151 MHz) δ (2D HSQC, HMBC) 169.5 (C, C-9'), 149.7 (C, C-3'), 146.8 (C, C-2'), 146.6 (CH, C-7'), 127.8 (C, C-6'), 122.9 (CH, C-5'), 116.6 (CH, C-4'), 115.3 (CH, C-8'), 115.1 (CH, C-1'), 65.6 (CH_2 , C-1), 33.2 (CH_2 , C-20), 30.9–30.0 (CH_2 , C-4–C-19), 29.9 (CH_2 , C-2), 27.1 (CH_2 , C-3), 23.7 (CH_2 , C-21), 14.4 (CH_3 , C-22)

Tetracosyl caffeate (**R8**): ^1H NMR (CD_3OD , 600 MHz) δ 7.53 (d, $J = 15.8$ Hz, 1H, H-7'), 7.04 (d, $J = 2.1$ Hz, 1H, H-1'), 6.94 (dd, $J = 8.0, 1.8$ Hz, 1H, H-5'), 6.78 (d, $J = 8.1$ Hz, 1H, H-4'), 6.25 (d, $J = 15.9$ Hz, 1H, H-8'), 4.17 (t, $J = 6.7$ Hz, 2H, H-1), 1.70 (p, $J = 6.9$ Hz, 2H, H-2), 1.40 (m, 2H, H-3), 1.29 (br s, 40H, H-4–H-23), 0.90 (t, $J = 6.8$ Hz, 3H, H-24)

Hexacosanyl caffeate (**R9**): ^1H NMR (CD_3OD , 600 MHz) for *O*-caffeoyl moiety δ 7.53 (d, $J = 15.7$ Hz, 1H, H-7'), 7.04 (d, $J = 2.1$ Hz, 1H, H-1'), 6.94 (dd, $J = 8.0, 1.8$ Hz, 1H, H-5'), 6.78 (d, $J = 8.2$ Hz, 1H, H-4'), 6.25 (d, $J = 15.8$ Hz, 1H, H-8')

2.4. Structure Elucidation of the Isolated Compounds

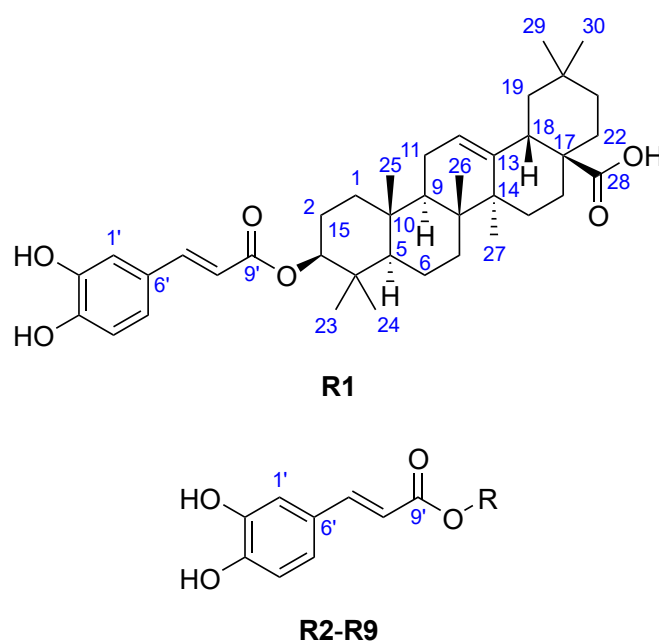
The NMR and ATR-FTIR spectroscopy data were consistent with HESI-HRMS data and in good agreement with the literature cited. The downfield region of the ^1H NMR spectra of

the isolated compounds **R1–R9** highly resembled each other with a set of resonances at δ_{H} 7.04–7.03 (d, $J \approx 2$ Hz, 1H, H-1'), 6.94 (dd, $J \approx 8$ and 2 Hz, 1H, H-5'), and 6.78 (d, $J \approx 8$ Hz, 1H, H-4') ppm suggesting the presence of a 1,2,4-trisubstituted aromatic ring. Moreover, ^1H signals at δ_{H} 7.53–7.52 (d, $J \approx 16$ Hz, 1H, H-7') and 6.25–6.24 (d, $J \approx 16$ Hz, 1H, H-8') ppm implied a *trans*-oriented, disubstituted carbon-carbon double bond. The ^{13}C or the ^1H - ^{13}C HMBC spectra of compounds **R1–R8** revealed one ester carbonyl carbon at δ_{C} 169.5–169.2 located at the C-9' position, as evidenced by HMBC correlations H-7'/C-9' and H-8'/C-9'. Besides, they exhibited typical carbon signals at δ_{C} 149.7–149.6 (C, C-3'), 146.9–146.7 (C, C-2'), 146.8–146.6 (CH, C-7'), 127.8–127.7 (C, C-6'), 123.0–122.9 (CH, C-5'), 116.6–116.5 (CH, C-4'), 115.6–115.2 (CH, C-8'), and 115.1 (CH, C-1') ppm, indicating that their structure contains an *O*-caffeoyl basic skeleton [28,29], which were corroborated by the ATR-FTIR absorption bands at around 3350–3200 cm^{-1} (O–H stretch) and at 1716–1710 cm^{-1} (α,β -unsaturated ester C=O stretch). The connectivity between the aromatic ring and the double bond was confirmed by long-range HMBC correlations H-8'/C-6', H-7'/C-1', H-7'/C-5', and H-7'/C-6'. The ^{13}C chemical shifts could not be determined for compounds **R6** and **R8** due to their low isolated quantity of below 1 mg (Table 1).

The HESI-HRMS spectrum of **R1** showed a deprotonated molecule peak at m/z 617.3848 $[\text{M}-\text{H}]^-$ establishing its molecular formula as $\text{C}_{39}\text{H}_{54}\text{O}_6$ (Table 1), which corresponded to 13 double bond equivalents. Its ^1H NMR spectrum (Table 2) indicated the presence of seven isolated methyl groups at δ_{H} 1.19 (s, 3H, H-27), 1.01 (s, 3H, H-25), 0.97 (s, 3H, H-24), 0.95 (s, 3H, H-30), 0.91 (s, 3H, H-23), 0.91 (s, 3H, H-29), and 0.84 (s, 3H, H-26) ppm, an olefinic proton at δ_{H} 5.26 (t, $J = 3.6$ Hz, 1H, H-12) ppm, and an oxymethine proton at δ_{H} 4.57 (dd, $J = 11.5, 4.3$ Hz, 1H, H-3) ppm. The ^{13}C NMR spectrum (Table 2) revealed 30 carbon resonances excluding the *O*-caffeoyl moiety, including seven methyl carbons at δ_{C} 33.6 (C-29), 28.7 (C-23), 26.4 (C-27), 24.0 (C-30), 17.7 (C-26), 17.3 (C-24), 15.9 (C-25) ppm, two olefinic carbons at δ_{C} 145.3 (C-13), 123.5 (C-12) ppm, one oxygenated carbon at δ_{C} 82.3 (C-3) ppm, as well as one carboxylic carbon at δ_{C} 182.1 (C-28) ppm. The caffeate and carboxylic moiety and the carbon-carbon double bond account for eight double bond equivalents, implying a pentacyclic triterpene skeleton with seven angular methyl groups. Based on the spectral data along with the 2D homo- and heteronuclear correlations and by comparing the ^1H , ^{13}C NMR, and ATR-FTIR data with those reported in the literature [30,31], the triterpene was identified as oleanolic acid. The point of attachment between the *O*-caffeoyl moiety and oleanolic acid was determined by the downfield chemical shifts of H-3 at δ_{H} 4.57 ppm and C-3 at δ_{C} 82.3 ppm, and a key HMBC correlation was observed from H-3 to C-9', supporting the substitution of oleanolic acid at the C-3 position. In addition, the large coupling constant between H-2_{ax} and H-3 ($^3J_{\text{H-2ax-H-3}} = 11.5$ Hz) confirmed that H-3 occupied an α -axial position, thereby indicating that the *O*-caffeoyl moiety was β -oriented. Thus, compound **R1** was elucidated as 3-*O*-caffeoyl oleanolic acid (Figure 3).

The ^1H NMR spectra of the four isolated compounds **R3**, **R5**, **R7**, and **R8** were remarkably similar, which was consistent with literature [32–36], displaying another set of signals at δ_{H} 4.17 (t, $J \approx 6.5$ Hz, 2H, H-1), 1.70 (p, $J \approx 7$ Hz, 2H, H-2), 1.41 (m, 2H, H-3), 1.29 (br s, varied integrals), 0.90 (t, $J \approx 7$ Hz, 3H, terminal CH_3) ppm suggestive for the presence of a saturated fatty acid moiety in their structures. It was verified by the observed ^{13}C signals at δ_{C} 65.6 (CH_2 , C-1), 33.2–33.1 (CH_2 , C-16(**R3**)/C-18(**R5**)/C-20(**R7**)), 30.9–30.0 (CH_2 , C-4–C-15(**R3**)/C-17(**R5**)/C-19(**R7**)), 29.9–29.8 (CH_2 , C-2), 27.1 (CH_2 , C-3), 23.7 (CH_2 , C-17(**R3**)/C-19(**R5**)/C-21(**R7**)), 14.4 (CH_3 , C-18(**R3**)/C-20(**R5**)/C-22(**R7**)) ppm [28,37]. In the HESI-HRMS spectra, deprotonated molecules were observed at m/z 431.3162 $[\text{M}-\text{H}]^-$ (**R3**), m/z 459.3475 $[\text{M}-\text{H}]^-$ (**R5**), m/z 487.3788 $[\text{M}-\text{H}]^-$ (**R7**), and m/z 515.4101 $[\text{M}-\text{H}]^-$ (**R8**), corresponding to the molecular formulae $\text{C}_{27}\text{H}_{44}\text{O}_4$ (**R3**), $\text{C}_{29}\text{H}_{48}\text{O}_4$ (**R5**), $\text{C}_{31}\text{H}_{52}\text{O}_4$ (**R7**), and $\text{C}_{33}\text{H}_{56}\text{O}_4$ (**R8**) (Table 1) that suspected a long-chain series with a two methylene group difference between adjacent members. The chemical formula of the aliphatic chains could be determined based on the fact that **R3**, **R5**, **R7**, and **R8** were caffeate esters: $\text{C}_{18}\text{H}_{37}$, $\text{C}_{20}\text{H}_{41}$, $\text{C}_{22}\text{H}_{45}$, and $\text{C}_{24}\text{H}_{49}$, respectively. Thus, the isolates were identified as octadecyl

caffeate (**R3**), eicosanyl caffeate (**R5**), docosyl caffeate (**R7**), and tetracosyl caffeate (**R8**), respectively (Figure 3).



Compound	R
R2	$-(\text{CH}_2)_8-\text{CH}=\text{CH}-(\text{CH}_2)_7-\text{CH}_3$
R3	$-(\text{CH}_2)_{17}-\text{CH}_3$
R4	$-(\text{CH}_2)_8-\text{CH}=\text{CH}-(\text{CH}_2)_9-\text{CH}_3$
R5	$-(\text{CH}_2)_{19}-\text{CH}_3$
R6	$-(\text{CH}_2)_8-\text{CH}=\text{CH}-(\text{CH}_2)_{11}-\text{CH}_3$
R7	$-(\text{CH}_2)_{21}-\text{CH}_3$
R8	$-(\text{CH}_2)_{23}-\text{CH}_3$
R9	$-(\text{CH}_2)_{25}-\text{CH}_3$

Figure 3. The chemical structures of the isolated compounds **R1–R9**.

Due to the low purity and isolated amount of compound **R9**, only limited structural information could be inferred from its ^1H NMR spectrum revealing the characteristic signals of *O*-caffeoyl moiety at δ_{H} 7.53 (d, $J = 15.7$ Hz, 1H, H-7'), 7.04 (d, $J = 1.8$ Hz, 1H, H-1'), 6.94 (dd, $J = 7.8$ and 1.9 Hz, 1H, H-5'), 6.78 (d, $J = 8.2$ Hz, 1H, H-4'), and 6.25 (d, $J = 15.8$ Hz, 1H, H-8') ppm. The HESI-HRMS spectrum displayed a deprotonated molecule peak at m/z 543.4419 $[\text{M}-\text{H}]^-$ indicating the molecular formula as $\text{C}_{35}\text{H}_{60}\text{O}_4$ (Table 1). Being a caffeate ester, the chemical formula $\text{C}_{26}\text{H}_{53}$ was deduced for the fatty alcohol moiety, thus compound **R9** was assigned as hexacosanyl caffeate (Figure 3) [38].

2.5. GC–MS for Assignment of the Double Bond Position

Based on the HESI-HRMS analyses (Table 1), deprotonated molecules were detected at m/z 429.3005 $[\text{M}-\text{H}]^-$ (**R2**), 457.3318 $[\text{M}-\text{H}]^-$ (**R4**), and m/z 485.3631 $[\text{M}-\text{H}]^-$ (**R6**), corresponding to the molecular formulae $\text{C}_{27}\text{H}_{42}\text{O}_4$ (**R2**), $\text{C}_{29}\text{H}_{46}\text{O}_4$ (**R4**), and $\text{C}_{31}\text{H}_{50}\text{O}_4$ (**R6**), indicative of one degree of unsaturation in the fatty alcohol moiety compared to **R3**, **R5**, **R7**, and **R8**. The ^1H NMR spectra of compounds **R2**, **R4**, and **R6** were similar to each other and that of **R3**, **R5**, **R7**, and **R8**, with the additional resonances at δ_{H} 5.34 (m, 2H) and 2.03 (m, 4H) consistent with one carbon-carbon double bond. The presence of a

monounsaturated long chain was supported by additional ^{13}C signals at δ_{C} 130.7–130.5 (CH) and 27.9–27.7 (CH₂) ppm, indicating the chemical formulae C₁₈H₃₅ (**R2**), C₂₀H₃₉ (**R4**), and C₂₂H₄₃ (**R6**) for aliphatic chains. However, the position of the double bond in the side chain could not be elucidated by NMR spectroscopy; therefore, GC–MS analyses were conducted. Compounds **R2** and **R4** were identified as oleyl and gadoleyl caffeate, respectively, as their aliphatic chains (oleyl and gadoleyl alcohol) were recognized by the NIST mass spectral library search, showing an excellent agreement between the experimental and theoretical EI-MS spectra (Figures S42 and S43). However, the long fatty alcohol chain of compound **R6** does not have a mass spectrum in the databases (Figure S44); therefore, we used its chromatographic retention property for its identification. The measured retention times for **R2**, **R4**, and **R6** were 7.5, 8.4, and 9.3 min, respectively (Figure S45). The identical position and configuration of the double bond (9Z) in the fatty alcohol chain of **R6** were confirmed by the linear relationship between the number of carbon atoms and logarithmic retention times ($R^2 = 0.998$) (Figure S46), indicating that **R2**, **R4**, and **R6** belong to the same homologous series. Thus, compound **R6** was determined as (Z)-9-docosenyl caffeate.

2.6. Equivalency Calculation of the Antioxidant Activity of the Isolates by DPPH• Microplate Assay

All isolated compounds exhibited antioxidant effects using the DPPH• microplate assay (Table 3), which confirmed the initial screening results obtained from the RP-HPTLC–DPPH• assay and the assignment by RP-HPTLC–HESI-HRMS. Antioxidant activity of **R1–R8** was compared to that of caffeic acid and found to be 0.10–0.35 mg caffeic acid equivalents per mg isolate, corresponding to 0.29–1.20 mol caffeic acid equivalents per mol isolate. The **R1** displayed the strongest antioxidant activity, surpassing caffeic acid at its molar level (1.20 mol caffeic acid equivalent/mol **R1**), while the **R8** demonstrated the weakest activity (0.29 mol caffeic acid equivalent/mol **R8**). The antioxidant effect of **R9** was detected but not quantified due to its low purity.

Table 3. Antioxidant activity of the isolated fatty alcohol caffeates expressed as caffeic acid equivalents (mean of triplicates with standard deviation SD).

Isolate	Mass Equivalency Caffeic Acid/Isolate (mg/mg ± SD)	Molar Equivalency Caffeic Acid/Isolate (mol/mol ± SD)
R1	0.35 ± 0.008	1.20 ± 0.024
R2	0.20 ± 0.005	0.49 ± 0.011
R3	0.19 ± 0.003	0.47 ± 0.007
R4	0.24 ± 0.002	0.61 ± 0.005
R5	0.26 ± 0.007	0.67 ± 0.018
R6	0.13 ± 0.003	0.35 ± 0.007
R7	0.17 ± 0.007	0.47 ± 0.021
R8	0.10 ± 0.003	0.29 ± 0.008

2.7. Progress Achieved in Comparison to Literature

3-O-Caffeoyl oleanolic acid (**R1**) has been isolated from different plant organs such as the seeds of *Oenothera biennis* [39], the whole plant of *Leptopus lolonum* [40], the leaves of *Elaeagnus oldhamii* [41], the barks of *Betula platyphylla* var. *japonica* [42], the skins of apples and pears [43], and the stem bark of *R. pseudoacacia* [44]. This compound demonstrated cytotoxic [41,45], antineoplastic [40,42], antibacterial against *Mycobacterium tuberculosis* [46], anti-inflammatory [43,47], anticoronavirus [45], and antioxidant [39] effects.

Phenolic esters with long-chain saturated fatty alcohols (**R3**, **R5**, **R7**, **R8**, and **R9**) were described in various plant species but not from the *Robinia* genus. Among others, the root bark of *Paeonia suffruticosa* [48], leaves of *Artemisia argyi* [49], bark of *Acacia*

species [50], and roots of *Ipomoea asarifolia* [51] were reported as a source of octadecyl caffeate (**R3**) that displayed α -glucosidase and α -amylase inhibition [48], antioxidant [36,49], cytotoxic [51], antiproliferative [37], anti-HIV (Human immunodeficiency virus) [52], and anti-inflammatory [37] activities. Eicosanyl caffeate (**R5**) and docosyl caffeate (**R7**) were found in stems of *Wikstroemia scytophylla* [53], roots of *Glycyrrhiza glabra* [33], and *Sophora* species [54,55]. Both exhibited chymotrypsin-like elastase inhibition [33], antiproliferative [37], anti-inflammatory [37], and antioxidant [33,49,56] effects. The isolation of docosyl caffeate (**R7**) from *Thymelaea hirsute* [57], the bark of *Acacia* species [50], its antineoplastic effect [57], and moderate activity against acetyl- and butyrylcholinesterase enzymes [58] have also been reported. Tetracosyl caffeate (**R8**) was described as a constituent of wigs of *Hypericum oblongifolium* [59], the whole plant of *Caragana conferta* [60], roots of *Caesalpinia mimosoides* [61], and bark of *Acacia* species [50], and as a urease inhibitor [62], anti-inflammatory [61], antineoplastic [34], antimicrobial [63], and cytotoxic [61] agent. The stem bark of *Pongamia glabra* [38], bark of *Acacia* species [50], stem bark and leaves of *Inga edulis* [64], and stems of *Hibiscus taiwanensis* [65] were sources of hexacosanyl caffeate (**R9**) that showed antioxidant activity [66]. Synthetic oleyl caffeate (**R2**) exerted inhibitory activity against HIV-1 [67]. To the best of our knowledge, oleyl caffeate (**R2**), gadoleyl caffeate (**R4**), and (*Z*)-9-docosenyl caffeate (**R6**) has not been reported previously as natural product constituents.

Phenolic compounds with hydrogen- or electron-donating properties are potential free radical scavengers that protect biomolecules from oxidative stress. Their antioxidant capacity is structure-related, mainly depending on the number and position of hydroxyl groups attached to the aromatic ring and the presence of sugar or other substituents [68]. Caffeic acid, with its dihydroxylated aromatic ring in *ortho* position, is one of the strongest phenolic antioxidants. Its half-maximal effective concentration (EC_{50}) value in the DPPH• assay was similar to that of flavonoid aglycones (quercetin, kaempferol, and epicatechin) and lower than that of the well-known potent antioxidant ascorbic acid or other phenolic acids (e.g., 3-*O*-chlorogenic acid, ferulic acid, *p*-coumaric acid, and *p*-hydroxybenzoic acid) [69,70]. In this study, the antioxidant activity of the isolated compounds was compared to that of caffeic acid, and it was found that 3-*O*-caffeoyl oleanolic acid (**R1**) was stronger, while other isolates were similar or slightly weaker than caffeic acid. These results are in agreement with literature data, as 3-*O*-caffeoyl oleanolic acid (**R1**) exerted lower free radical scavenging activity than ascorbic acid [39], octadecyl caffeate (**R3**) showed an antioxidant effect comparable to caffeic acid and higher than ferulic acid and sinapic acid [36], and hexacosanyl caffeate (**R9**) exhibited a slightly lower activity than caffeic acid [66]. However, in the DPPH• assay, eicosanyl caffeate (**R5**) and docosyl caffeate (**R7**) displayed weaker antioxidant activity (10–15 times higher EC_{50}) than gallic acid [33,49], which was found to be a stronger free radical scavenger (two times lower EC_{50}) than caffeic acid in the same assay [71].

3. Materials and Methods

3.1. Materials

HPTLC plates, silica gel 60 RP18, and methanol (MS grade) were purchased from Merck (Darmstadt, Germany). Solvents for extraction and HPTLC (analytical grade) were obtained from Th. Geyer (Renningen, Germany) or Reanal (Budapest, Hungary). The 2,2-diphenyl-1-picrylhydrazyl radical (DPPH•) and caffeic acid (98%) were acquired from Sigma-Aldrich (Steinheim, Germany), and Natural Product reagent A (diphenylboryloxyethylamine or diphenylboric acid β -ethylamino ester, 98%) was purchased from Carl Roth (Karlsruhe, Germany). Methanol- d_4 (CD_3OD , 99.8 atom% D) for NMR measurements was purchased from VWR (Budapest, Hungary), and gradient-grade methanol and acetonitrile for isolation were supplied by Fisher Scientific (Pittsburg, PA, USA).

3.2. Sample Origin and Preparation

The stem bark of *R. pseudoacacia* L. was collected in October 2016 in Harta (46°41'45" N 19°02'26" E, altitude: 93 m) in the Great Plain of Hungary and dried at room temperature. A voucher sample (PPI-MA-RB1) has been deposited at the herbarium of the Plant Protection Institute, Centre for Agricultural Research, Budapest, Hungary. The dried material was powdered by a coffee grinder (Bosch MKM6000, Stuttgart, Germany) and was extracted with methanol (150 mg/mL) using an ultrasound-assisted extraction for 10 min (Sonorex Super RK 106, Bandelin, Berlin, Germany) and centrifuged for 1 min at 5000 × *g* (Dlab D1008, Beijing, China).

3.3. High-Performance Thin-Layer Chromatography, Derivatization, and DPPH• Assay

The crude extract (3 µL) was applied onto the RP18 HPTLC plate by the Automatic TLC Sampler 4 (ATS4, CAMAG, Muttenz, Switzerland) as a 7 mm band with an 8 mm distance from the lower edge. HPTLC separation was carried out with a mobile phase of acetonitrile—ethanol 3:2 *V/V* in a Twin Trough Chamber (10 cm × 10 cm, CAMAG) up to 80 mm from the lower edge of the plate. The dried chromatogram was detected at 254 nm and 365 nm with the TLC Visualizer (CAMAG), and the UV spectra of selected zones were recorded by a TLC Scanner 4 (CAMAG). To detect phenolics (e.g., flavonoids, anthocyanidines, hydroxyl- and methoxycinnamic acids [72]), the plate was dipped into a 0.5% methanolic solution of Natural Product reagent A, dried, and documented at 365 nm. Free radical scavenging activity was visualized by the HPTLC–DPPH• assay. The chromatogram was immersed into a 0.02% methanolic solution of DPPH•, and the bright zones of antioxidants against a lilac background were documented under white light illumination in the transmittance mode (TLC Visualizer).

3.4. HPTLC–HESI–HRMS

For HPTLC–HRMS analysis [73,74], a TLC–MS Interface (CAMAG) or a PlateExpress interface (Advion, Ithaca, NY, USA) equipped with an oval elution head (4 mm × 2 mm) was integrated online between a quaternary pump (Ultimate LPG-3400 XRS, Dionex Softron, Germering, Germany) and a hybrid quadrupole-orbitrap mass spectrometer operated with a heated electrospray ionization probe (HESI-II, Q Exactive Plus, Thermo Fisher Scientific, Bremen, Germany). MS-grade methanol at a flow rate of 0.1 mL/min was used to elute selected zones. The following conditions were applied: spray voltage 3.5 kV, capillary temperature 270 °C, and nitrogen sheath and auxiliary gas with 20 and 10 arbitrary units, respectively, produced by an SF2 compressor (Atlas Copco Kompressoren und Drucklufttechnik, Essen, Germany). HRMS full scan spectra were recorded in both negative and positive ionization modes in the range of *m/z* 80–1200 with a resolution of 280,000; the automatic gain control target (AGCT) was set to 3 × 10⁶, and the maximum injection time (IT) was 100 ms. Xcalibur 3.0.63 software (Thermo Fisher Scientific) provided the instrument control and data analysis.

3.5. Fractionation by Solid-Phase Extraction

The bark powder (20 g) was extracted three times with 100 mL of methanol by ultrasound-assisted extraction. The combined extracts were filtered (Whatman No. 2 filter paper, Sigma), concentrated by a rotary evaporator to 20 mL (Büchi Rotavapor R-134, Flawil, Switzerland), and diluted with water to 40 mL. This methanol-water 1:1 crude extract was purified by solid-phase extraction using Strata-XL cartridges (10 portions, 200 mg 100 µm polymeric RP, Phenomenex, Torrance, CA, USA). The cartridge was rinsed with 4 mL of methanol, conditioned with 4 mL of 50% aqueous methanol, loaded with 4 mL of sample, washed with 4 mL of acetonitrile, and then eluted with 4 mL of ethanol. The whole 10 eluates (from 10 cartridges) were pooled, concentrated by a rotary evaporator to 2 mL, and transferred to HPLC analysis.

3.6. Compound Isolation by HPLC–DAD–ESI–MS

The antioxidant compounds were isolated by HPLC using an LCMS-2020 system (Shimadzu, Kyoto, Japan) consisting of a binary gradient solvent pump, a vacuum degasser, a thermostated autosampler, a column oven, a photodiode detector, and a mass analyzer using an electrospray ionization (ESI) interface. The instrument control, data acquisition, and data processing were carried out by LabSolutions 5.42v software (Shimadzu). Separation was achieved on a Gemini C₁₈ column (250 mm length, 4.6 mm ID, 5 µm particle size, Phenomenex, Torrance, CA, USA) at 35 °C with a linear gradient of 5% aqueous acetonitrile with 0.05% formic acid (A) and methanol with 0.05% formic acid (B). The gradient program was as follows: 0–16 min, 92% B; 16–25 min, 92–100% B; 25–35 min, 100% B; and 35.1–40 min, 92% B. The flow rate of the mobile phase was adjusted to 1.2 mL/min. The injection volume was set to 1 µL for method development and 100 µL for isolation. The appropriate peaks were collected based on the UV chromatogram at 323 nm, and the fractionation protocol was repeated 15 times. The combined 15 fractions were dried with a rotary evaporator at 40 °C and transferred to NMR spectroscopy. The MS conditions were as follows: nebulizer gas (N₂) flow rate 1.5 L/min, drying gas (N₂) flow rate 15 L/min, interface temperature 350 °C, heat block temperature 400 °C, desolvation line temperature 250 °C, and detector voltage 4.5 kV. Full mass scan spectra were recorded in the negative ionization mode in the range of *m/z* 150–1000 with a scan speed of 883 u/s.

3.7. NMR Spectroscopy

The isolated compounds **R1–R9** were dissolved in methanol-*d*₄, and the samples were transferred to a standard 5 mm NMR tube for measurements. NMR spectra were collected on a Varian DDR 600 (¹H: 599.9 MHz, ¹³C: 150.9 MHz; 14.1 T) spectrometer equipped with a dual 5 mm inverse-detection pulsed-field gradient (IDPFG) probehead at 298 K. The instrument was operated and controlled by VnmrJ 3.2C software. All applied pulse sequences were obtained from the Chempack 5.1 standard pulse program library of the instrument. ¹H and ¹³C chemical shifts (δ) are provided on the δ -scale, reported in ppm and referenced to the NMR solvent used (CHD₂OD residual peak at $\delta_{\text{H}} = 3.31$ ppm and CD₃OD at $\delta_{\text{C}} = 49.0$ ppm), whereas spin-spin coupling constants (*J*) are given in Hz. The signal multiplicities are denoted as s—singlet, br s—broad singlet, d—doublet, t—triplet, p—pentet; m—multiplet; dd—doublet of doublets; td—triplet of doublets. The full ¹H and ¹³C NMR resonance assignments were performed by means of comprehensive one- (¹H and ¹³C) and two-dimensional homonuclear (¹H–¹H COSY and ¹H–¹H TOCSY) and heteronuclear (¹H–¹³C edHSQC (¹*J*_{C–H} = 140 Hz) and ¹H–¹³C HMBC (^{*n*}*J*_{C–H} = 8 Hz), both of them gradient-enhanced with adiabatic pulses) NMR experiments. In the case of compound **1**, band-selective HSQC (bsHSQC) and HMBC (bsHMBC) spectra were also recorded to enhance the spectral resolution in the F1 dimension.

3.8. ATR-FTIR Spectroscopy

The ATR-FTIR spectra were recorded by a Perkin Elmer Spectrum 400 FT-IR/FT-NIR spectrometer (Waltham, MA, USA) equipped with a diamond/ZnSe ATR crystal and a MIR TGS detector. Spectra were collected in the range of 4000–650 cm^{−1} with a spectral resolution of 4 cm^{−1}. A few drops of the isolates (1 mg/mL in ethanol) were placed onto the ATR crystal, then the solvent was completely evaporated and the spectra were obtained by averaging 8–32 scans after background subtraction. Data processing and analysis were performed by Perkin Elmer Spectrum Software version 6.3.1, which included baseline correction and Savitzky-Golay smoothing.

3.9. GC–MS

The isolated compounds **R2**, **R4**, and **R6** were dissolved in ethanol (1 mg/mL). For the GC–MS analysis, a Shimadzu GCMS-TQ8040 NX instrument was applied using a Rtx-5 (30 m × 250 µm i.d.; film thickness: 0.32 µm, Restek, Bellefonte, PA, USA) capillary column. Helium was used as a carrier gas with a linear velocity of 50 cm/s. The solution of each

compound (1 μ L) was injected in split mode (split ratio 1:20) at 300 °C. The column oven temperature was programmed to increase from 80 °C to 320 °C at 20 °C/min, and the final temperature was held for 10.5 min. The ionization in the electron impact ion source was performed with an electron beam of 70 eV. The triple quadrupole analyzer operated in full scan mode (m/z range 29–600, scan speed 3333 amu/s). The interface and the ion source temperatures were maintained at 280 °C, and the accelerating and detector voltages were set to 4.0 kV and 0.9 kV, respectively. The data were acquired and evaluated with GCMSolutions 4.52 software (Shimadzu). The identification of the compounds was aided by the NIST 17 mass spectral library.

3.10. DPPH• Microplate Assay of Isolated Compounds

The antioxidant activity of the isolated compounds (1 mg/mL in ethanol) was evaluated using 96-well microplates and expressed as caffeic acid equivalents (mg caffeic acid/mg isolates and mol caffeic acid equivalent/mol isolates). Caffeic acid (10, 9, 8, 7, 6, 5, 4, 3, 2, 1 μ L, 1 mg/mL in ethanol) and isolated compounds (10 μ L) were pipetted to the wells in triplicate (on two separate occasions). After evaporation of the ethanol, 100 μ L of DPPH• solution (0.3 M in methanol) was added to each well. After incubating the microplate at 25 °C for 10 min in the dark, the deep-violet stable free radical DPPH• was reduced to the pale-yellow 2,2-diphenyl-1-picrylhydrazine in the presence of antioxidants, resulting in a decrease in absorbance measured at 517 nm (Clariostar® Plus microplate reader, BMG LABTECH, Ortenberg, Germany).

4. Conclusions

This study identified nine antioxidant caffeate esters from the stem bark of *R. pseudoacacia* using RP-HPTLC–DPPH• assay, RP-HPTLC–UV/VIS/FLD–HESI–HRMS, HPLC–DAD–ESI–MS, GC–MS, ATR–FTIR, and NMR spectroscopy. It led to the identification of 3-*O*-caffeoyl oleanolic acid (**R1**), oleyl caffeate (**R2**), octadecyl caffeate (**R3**), gadoleyl caffeate (**R4**), eicosanyl caffeate (**R5**), (*Z*)-9-docosenyl caffeate (**R6**), docosyl caffeate (**R7**), tetracosyl caffeate (**R8**), and hexacosanyl caffeate (**R9**). This is the first report for natural compounds **R2**, **R4**, and **R6**, while **R3**, **R5**, **R7**, **R8**, and **R9** were obtained from this genus for the first time. The antioxidant effects of the isolated compounds were confirmed using the DPPH• microplate assay. The stem bark of black locust holds significant potential as a candidate for pharmaceutical applications, as the known isolates display a range of other bioactivities such as antimicrobial, cytotoxic, antiproliferative, and anti-inflammatory properties.

Supplementary Materials: The following supporting information can be downloaded at: <https://www.mdpi.com/article/10.3390/molecules29235673/s1>, Figure S1: UV–VIS spectra (190–600 nm) of the compounds **R1–R9** recorded by RP–HPTLC–densitometry; Figure S2: HPTLC chromatogram of black locust bark isolates (**R1–R9**) and extract (**E**) on RP18 plates with acetonitrile–ethanol 3:2 *V/V* after derivatization with natural product reagent at UV 365 nm; Figures S3–S35: 1D and 2D NMR spectra of compounds **R1–R9**; Figures S36–S41: ATR FTIR spectra of compounds **R1–R7**; Figure S42: The experimental EI–MS spectrum of compound **R2** and the theoretical EI–MS spectrum of oleyl alcohol; Figure S43: The experimental EI–MS spectrum of compound **R4** and the theoretical EI–MS spectrum of gadoleyl alcohol; Figure S44: The experimental EI–MS spectrum of compound **R6**; Figure S45: GC–MS TIC chromatograms of compounds **R2**, **R4**, and **R6**; Figure S46: Plot of the logarithmic retention time (t_R) versus the number of carbon atoms for compounds **R2**, **R4**, and **R6**.

Author Contributions: Conceptualization, resources, and writing—review and editing, Á.M.M. and G.E.M.; methodology, and investigation, Á.M.M.; data curation, and writing—original draft preparation, M.B. and Á.M.M.; A.D. performed the spectral analyses; J.B. performed the GC–MS analyses. All authors have read and agreed to the published version of the manuscript.

Funding: This work was partially funded by the National Research, Development, and Innovation Office of Hungary (SNN139496, Á.M.M.). Instrumentation at JLU Giessen was partially funded by the Deutsche Forschungsgemeinschaft (DFG, German Research Foundation)—INST 162/471-1 FUGG; INST 162/536-1 FUGG.

Institutional Review Board Statement: Not applicable.

Informed Consent Statement: Not applicable.

Data Availability Statement: Data are available upon reasonable request.

Acknowledgments: The authors express their gratitude to Judit Nyiri (Pharmaceutical Chemistry and Technology Department, National Institute of Pharmacy and Nutrition, Budapest, Hungary) for her assistance in recording the ATR-FTIR spectra.

Conflicts of Interest: The authors declare no conflicts of interest.

References

1. Puchałka, R.; Dyderski, M.K.; Vítková, M.; Sádlo, J.; Klisz, M.; Netsvetov, M.; Prokopuk, Y.; Matison, R.; Mionskowski, M.; Wojda, T.; et al. Black Locust (*Robinia pseudoacacia* L.) Range Contraction and Expansion in Europe under Changing Climate. *Glob. Chang. Biol.* **2021**, *27*, 1587–1600. [[CrossRef](#)] [[PubMed](#)]
2. Csiszár, Á.; Winkler, D.; Bartha, D.; Zagyvai, G. Diverse Interactions: Root-Nodule Formation and Herb-Layer Composition in Black Locust (*Robinia pseudoacacia*) Stands. *Plants* **2023**, *12*, 3253. [[CrossRef](#)]
3. Botta-Dukat, Z.; Balogh, L.; Feher, A. *The Most Important Invasive Plants in Hungary*; Institute of Ecology and Botany; Hungarian Academy of Sciences: Budapest, Hungary, 2008.
4. Vítková, M.; Müllerová, J.; Sádlo, J.; Pergl, J.; Pyšek, P. Black Locust (*Robinia pseudoacacia*) Beloved and Despised: A Story of an Invasive Tree in Central Europe. *For. Ecol. Manage.* **2017**, *384*, 287–302. [[CrossRef](#)]
5. Motti, R.; Paura, B.; Cozzolino, A.; de Falco, B. Edible Flowers Used in Some Countries of the Mediterranean Basin: An Ethnobotanical Overview. *Plants* **2022**, *11*, 3272. [[CrossRef](#)]
6. Zhang, Y.; Yang, S.; Zhao, X.; Yang, Y.; Li, B.; Zhu, F.; Zhu, R. Immune Enhancement of Taishan *Robinia pseudoacacia* Polysaccharide on Recombinant Proteus Mirabilis OmpA in Chickens. *Int. Immunopharmacol.* **2014**, *22*, 236–241. [[CrossRef](#)] [[PubMed](#)]
7. Patra, J.; Kim, E.; Oh, K.; Kim, H.-J.; Dhakal, R.; Kim, Y.; Baek, K.-H. Bactericidal Effect of Extracts and Metabolites of *Robinia pseudoacacia* L. on *Streptococcus mutans* and *Porphyromonas gingivalis* Causing Dental Plaque and Periodontal Inflammatory Diseases. *Molecules* **2015**, *20*, 6128–6139. [[CrossRef](#)] [[PubMed](#)]
8. Hallmann, E. Quantitative and Qualitative Identification of Bioactive Compounds in Edible Flowers of Black and Bristly Locust and Their Antioxidant Activity. *Biomolecules* **2020**, *10*, 1603. [[CrossRef](#)]
9. Uzelac, M.; Sladonja, B.; Šola, I.; Dudaš, S.; Bilić, J.; Famuyide, I.M.; McGaw, L.J.; Eloff, J.N.; Mikulic-Petkovsek, M.; Poljuha, D. Invasive Alien Species as a Potential Source of Phytopharmaceuticals: Phenolic Composition and Antimicrobial and Cytotoxic Activity of *Robinia pseudoacacia* L. Leaf and Flower Extracts. *Plants* **2023**, *12*, 2715. [[CrossRef](#)]
10. Obistioiu, D.; Cocan, I.; Tîrziu, E.; Herman, V.; Negrea, M.; Cucerzan, A.; Neacsu, A.-G.; Cozma, A.L.; Nichita, I.; Hulea, A.; et al. Phytochemical Profile and Microbiological Activity of Some Plants Belonging to the Fabaceae Family. *Antibiotics* **2021**, *10*, 662. [[CrossRef](#)]
11. Truchado, P.; Ferreres, F.; Bortolotti, L.; Sabatini, A.G.; Tomás-Barberán, F.A. Nectar Flavonol Rhamnosides Are Floral Markers of Acacia (*Robinia pseudacacia*) Honey. *J. Agric. Food Chem.* **2008**, *56*, 8815–8824. [[CrossRef](#)]
12. Tian, F.; Chang, C.-J.; Grutzner, J.B.; Nichols, D.E.; McLaughlin, J.L. Robinlin: A Novel Bioactive Homo-Monoterpene from *Robinia pseudoacacia* L. (Fabaceae). *Bioorg. Med. Chem. Lett.* **2001**, *11*, 2603–2606. [[CrossRef](#)] [[PubMed](#)]
13. Amorim, C.; Silvério, S.C.; Prather, K.L.J.; Rodrigues, L.R. From Lignocellulosic Residues to Market: Production and Commercial Potential of Xylooligosaccharides. *Biotechnol. Adv.* **2019**, *37*, 107397. [[CrossRef](#)] [[PubMed](#)]
14. Kamperidou, V.; Terzopoulou, P.; Barboutis, I. Marginal Lands Providing Tree-crop Biomass as Feedstock for Solid Biofuels. *Biofuels Bioprod. Biorefining* **2021**, *15*, 1395–1405. [[CrossRef](#)]
15. Pérez-Pérez, A.; Gullón, B.; Lobato-Rodríguez, Á.; Garrote, G.; del Río, P.G. Microwave-Assisted Extraction of Hemicellulosic Oligosaccharides and Phenolics from *Robinia pseudoacacia* Wood. *Carbohydr. Polym.* **2023**, *301*, 120364. [[CrossRef](#)]
16. Sergeant, T.; Kohnen, S.; Jourez, B.; Beauve, C.; Schneider, Y.-J.; Vincke, C. Characterization of Black Locust (*Robinia pseudoacacia* L.) Heartwood Extractives: Identification of Resveratrol and Piceatannol. *Wood Sci. Technol.* **2014**, *48*, 1005–1017. [[CrossRef](#)]
17. Vek, V.; Poljanšek, I.; Oven, P. Efficiency of Three Conventional Methods for Extraction of Dihydrorobinetin and Robinetin from Wood of Black Locust. *Eur. J. Wood Wood Prod.* **2019**, *77*, 891–901. [[CrossRef](#)]
18. Magel, E.; Jay-Allemand, C.; Ziegler, H. Formation of Heartwood Substances in the Stemwood of *Robinia pseudoacacia* L. II. Distribution of Nonstructural Carbohydrates and Wood Extractives across the Trunk. *Trees* **1994**, *8*, 165–171. [[CrossRef](#)]
19. Putman, L.J.; Laks, P.E.; Pruner, M.S. Chemical Constituents of Black Locust Bark and Their Biocidal Activity. *Holzforschung* **1989**, *43*, 219–224. [[CrossRef](#)]
20. Dai, J.; Mumper, R.J. Plant Phenolics: Extraction, Analysis and Their Antioxidant and Anticancer Properties. *Molecules* **2010**, *15*, 7313–7352. [[CrossRef](#)] [[PubMed](#)]
21. Khalid, M.; Saeed-ur-Rahman; Bilal, M.; Huang, D. Role of Flavonoids in Plant Interactions with the Environment and against Human Pathogens—A Review. *J. Integr. Agric.* **2019**, *18*, 211–230. [[CrossRef](#)]

22. Zhang, C.; Jia, X.; Zhao, Y.; Wang, L.; Wang, Y. Adaptive Response of Flavonoids in *Robinia pseudoacacia* L. Affected by the Contamination of Cadmium and Elevated CO₂ to Arbuscular Mycorrhizal Symbiosis. *Ecotoxicol. Environ. Saf.* **2023**, *263*, 115379. [[CrossRef](#)] [[PubMed](#)]
23. Zeb, A. Concept, Mechanism, and Applications of Phenolic Antioxidants in Foods. *J. Food Biochem.* **2020**, *44*, e13394. [[CrossRef](#)] [[PubMed](#)]
24. Krüger, S.; Urmann, O.; Morlock, G.E. Development of a Planar Chromatographic Method for Quantitation of Anthocyanes in Pomace, Feed, Juice and Wine. *J. Chromatogr. A* **2013**, *1289*, 105–118. [[CrossRef](#)] [[PubMed](#)]
25. Krüger, S.; Hüsken, L.; Fornasari, R.; Scainelli, I.; Morlock, G.E. Effect-Directed Fingerprints of 77 Botanical Extracts via a Generic High-Performance Thin-Layer Chromatography Method Combined with Assays and Mass Spectrometry. *J. Chromatogr. A* **2017**, *1529*, 93–106. [[CrossRef](#)] [[PubMed](#)]
26. Inarejos-Garcia, A.M.; Heil, J.; Martorell, P.; Álvarez, B.; Llopis, S.; Helbig, I.; Liu, J.; Quebbeman, B.; Nemeth, T.; Holmgren, D.; et al. Effect-Directed, Chemical and Taxonomic Profiling of Peppermint Proprietary Varieties and Corresponding Leaf Extracts. *Antioxidants* **2023**, *12*, 476. [[CrossRef](#)]
27. Móricz, Á.M.; Ott, P.G.; Häbe, T.T.; Darcsi, A.; Böszörményi, A.; Alberti, Á.; Krüzselyi, D.; Csontos, P.; Béni, S.; Morlock, G.E. Effect-Directed Discovery of Bioactive Compounds Followed by Highly Targeted Characterization, Isolation and Identification, Exemplarily Shown for *Solidago virgaurea*. *Anal. Chem.* **2016**, *88*, 8202–8209. [[CrossRef](#)] [[PubMed](#)]
28. Uwai, K.; Osanai, Y.; Imaizumi, T.; Kanno, S.; Takeshita, M.; Ishikawa, M. Inhibitory Effect of the Alkyl Side Chain of Caffeic Acid Analogues on Lipopolysaccharide-Induced Nitric Oxide Production in RAW264.7 Macrophages. *Bioorg. Med. Chem.* **2008**, *16*, 7795–7803. [[CrossRef](#)]
29. Zhang, W.-D.; Bang Tam, H.T.; Chen, W.-S.; Kong, D.-Y.; Li, H.-T.; Wang, Y.-H.; Fouraste, I. Two New Caffeoyl Conjugation from *Erigeron breviscapus*. *J. Asian Nat. Prod. Res.* **2000**, *2*, 283–288. [[CrossRef](#)]
30. Marealle, A.I.; Innocent, E.; Andrae-Marobela, K.; Qwarse, M.; Machumi, F.; Nondo, R.S.O.; Heydenreich, M.; Moshi, M.J. Safety Evaluation and Bioassay-Guided Isolation of Antimycobacterial Compounds from *Morella salicifolia* Root Ethanolic Extract. *J. Ethnopharmacol.* **2022**, *296*, 115501. [[CrossRef](#)]
31. Pan, H.; Lundgren, L.N.; Andersson, R. Triterpene Caffeates from Bark of *Betula pubescens*. *Phytochemistry* **1994**, *37*, 795–799. [[CrossRef](#)]
32. Menezes, J.C.J.M.D.S.; Edraki, N.; Kamat, S.P.; Khoshneviszadeh, M.; Kayani, Z.; Mirzaei, H.H.; Miri, R.; Erfani, N.; Nejati, M.; Cavaleiro, J.A.S.; et al. Long Chain Alkyl Esters of Hydroxycinnamic Acids as Promising Anticancer Agents: Selective Induction of Apoptosis in Cancer Cells. *J. Agric. Food Chem.* **2017**, *65*, 7228–7239. [[CrossRef](#)] [[PubMed](#)]
33. Dey, S.; Deepak, M.; Setty, M.; D'Souza, P.; Agarwal, A.; Sangli, G.K. Bioactive Caffeic Acid Esters from *Glycyrrhiza glabra*. *Nat. Prod. Res.* **2009**, *23*, 1657–1663. [[CrossRef](#)] [[PubMed](#)]
34. Velazquez Cruz, M.; Salinas-Arellano, E.; Castro Dionicio, I.; Jeyaraj, J.G.; Mirtallo Ezzone, N.P.; Carcache de Blanco, E.J. Bioactive Compounds Isolated from the Bark of *Aesculus glabra* Willd. *Phytochem. Lett.* **2024**, *61*, 106–114. [[CrossRef](#)] [[PubMed](#)]
35. Tabakam, G.T.; Kodama, T.; Donfack, A.R.N.; Nguekeu, Y.M.M.; Nomin-Erdene, B.; Htoo, Z.P.; Do, K.M.; Ngouela, S.A.; Tene, M.; Morita, H.; et al. A New Caffeic Acid Ester and a New Ceramide from the Roots of *Eriosema glomeratum*. *Phytochem. Lett.* **2021**, *45*, 82–87. [[CrossRef](#)]
36. Menezes, J.C.J.M.D.S.; Kamat, S.P.; Cavaleiro, J.A.S.; Gaspar, A.; Garrido, J.; Borges, F. Synthesis and Antioxidant Activity of Long Chain Alkyl Hydroxycinnamates. *Eur. J. Med. Chem.* **2011**, *46*, 773–777. [[CrossRef](#)] [[PubMed](#)]
37. Jayaprakasam, B.; Vanisree, M.; Zhang, Y.; Dewitt, D.L.; Nair, M.G. Impact of Alkyl Esters of Caffeic and Ferulic Acids on Tumor Cell Proliferation, Cyclooxygenase Enzyme, and Lipid Peroxidation. *J. Agric. Food Chem.* **2006**, *54*, 5375–5381. [[CrossRef](#)]
38. Saha, M.M.; Mallik, U.K.; Mallik, A.K. A Chromenoflavanone and Two Caffeic Esters from *Pongamia glabra*. *Phytochemistry* **1991**, *30*, 3834–3836. [[CrossRef](#)]
39. Hamburger, M.; Riese, U.; Graf, H.; Melzig, M.F.; Ciesielski, S.; Baumann, D.; Dittmann, K.; Wegner, C. Constituents in Evening Primrose Oil with Radical Scavenging, Cyclooxygenase, and Neutrophil Elastase Inhibitory Activities. *J. Agric. Food Chem.* **2002**, *50*, 5533–5538. [[CrossRef](#)]
40. Qi, S.-Z.; Liu, T.; Wang, M.; Zhang, X.-X.; Yang, Y.-R.; Jing, W.-H.; Long, L.-P.; Song, K.-R.; Jin, Y.; Gao, H.-Y. New Phenylpropanoid-Conjugated Pentacyclic Triterpenoids from the Whole Plants of *Leptopus lolonum* with Their Antiproliferative Activities on Cancer Cells. *Bioorg. Chem.* **2021**, *107*, 104628. [[CrossRef](#)]
41. Liao, C.-R.; Kuo, Y.-H.; Ho, Y.-L.; Wang, C.-Y.; Yang, C.; Lin, C.-W.; Chang, Y.-S. Studies on Cytotoxic Constituents from the Leaves of *Elaeagnus oldhamii* Maxim. in Non-Small Cell Lung Cancer A549 Cells. *Molecules* **2014**, *19*, 9515–9534. [[CrossRef](#)]
42. Eom, H.J.; Kang, H.R.; Choi, S.U.; Kim, K.H. Cytotoxic Triterpenoids from the Barks of *Betula platyphylla* var. *japonica*. *Chem. Biodivers.* **2017**, *14*, e1600400. [[CrossRef](#)] [[PubMed](#)]
43. Andre, C.M.; Larsen, L.; Burgess, E.J.; Jensen, D.J.; Cooney, J.M.; Evers, D.; Zhang, J.; Perry, N.B.; Laing, W.A. Unusual Immunomodulatory Triterpene-Caffeates in the Skins of Russeted Varieties of Apples and Pears. *J. Agric. Food Chem.* **2013**, *61*, 2773–2779. [[CrossRef](#)] [[PubMed](#)]
44. Zarev, Y. Isolation and Characterization of 3- O-Caffeoyloleanolic Acid from *Robinia pseudoacacia* Stem Bark. *Pharmacia* **2023**, *70*, 1209–1212. [[CrossRef](#)]

45. Al Ibrahim, M.; Akissi, Z.L.E.; Desmarests, L.; Lefèvre, G.; Samaille, J.; Raczkiwicz, I.; Sahpaz, S.; Dubuisson, J.; Belouzard, S.; Rivière, C.; et al. Discovery of Anti-Coronavirus Cinnamoyl Triterpenoids Isolated from *Hippophae rhamnoides* during a Screening of Halophytes from the North Sea and Channel Coasts in Northern France. *Int. J. Mol. Sci.* **2023**, *24*, 16617. [[CrossRef](#)] [[PubMed](#)]
46. Tanachatchairatana, T.; Bremner, J.B.; Chokchaisiri, R.; Suksamrarn, A. Antimycobacterial Activity of Cinnamate-Based Esters of the Triterpenes Betulinic, Oleanolic and Ursolic Acids. *Chem. Pharm. Bull.* **2008**, *56*, 194–198. [[CrossRef](#)] [[PubMed](#)]
47. Yang, Z.-G.; Li, H.-R.; Wang, L.-Y.; Li, Y.-H.; Lu, S.-G.; Wen, X.-F.; Wang, J.; Daikonya, A.; Kitanaka, S. Triterpenoids from *Hippophae rhamnoides* L. and Their Nitric Oxide Production-Inhibitory and DPPH Radical-Scavenging Activities. *Chem. Pharm. Bull.* **2007**, *55*, 15–18. [[CrossRef](#)]
48. Chen, P.-C.; Dlamini, B.S.; Chen, C.-R.; Shih, W.-L.; Lee, C.-H.; Chang, C.-I. Inhibitory Potential of Chemical Constituents from *Paeonia suffruticosa* Against α -Glucosidase and α -Amylase. *Pharm. Chem. J.* **2022**, *56*, 821–826. [[CrossRef](#)]
49. Lv, J.; Duan, J.; Shen, B.; Yin, Y. Caffeic Acid Esters from *Artemisia argyi* and Their Antioxidant Activities. *Chem. Nat. Compd.* **2013**, *49*, 8–11. [[CrossRef](#)]
50. Freire, C.S.R.; Silvestre, A.J.D.; Neto, C.P. Demonstration of Long-chain *n*-Alkyl Caffeates and Δ^7 -steryl Glucosides in the Bark of *Acacia* Species by Gas Chromatography–Mass Spectrometry. *Phytochem. Anal.* **2007**, *18*, 151–156. [[CrossRef](#)]
51. Saraux, N.; Imeri, D.; Quirós-Guerrero, L.; Karimou, S.; Christen, P.; Cuendet, M. Phytochemical Investigation of the Roots of *Ipomoea asarifolia* and Antiproliferative Activity of the Isolated Compounds against Multiple Myeloma Cells. *J. Nat. Prod.* **2022**, *85*, 56–62. [[CrossRef](#)]
52. Huang, S.; Zhang, X.; Li, X.; Jiang, H.; Ma, Q.; Wang, P.; Liu, Y.; Hu, J.; Zheng, Y.; Zhou, J.; et al. Phenols with Anti-HIV Activity from *Daphne acutiloba*. *Planta Med.* **2012**, *78*, 182–185. [[CrossRef](#)] [[PubMed](#)]
53. Jiang, H.; Ma, Q.; Huang, S.; Liang, W.; Wang, P.; Hu, J.; Zhou, J.; Zhao, Y. A New Guaiane-type Sesquiterpene with 15 Known Compounds from *Wikstroemia scytophylla* Diels. *Chin. J. Chem.* **2012**, *30*, 1335–1338. [[CrossRef](#)]
54. Komatsu, M.; Yokoe, I.; Shirataki, Y. Studies on the Constituents of *Sophora* Species. XIII. Constituents of the Aerial Parts of *Sophora tomentosa* L. *Chem. Pharm. Bull.* **1978**, *26*, 3863–3870. [[CrossRef](#)] [[PubMed](#)]
55. Inuma, M.; Tanaka, T.; Mizuno, M.; Lang, F.A. Two Flavanones from Roots of *Sophora leachiana*. *Phytochemistry* **1992**, *31*, 721–723. [[CrossRef](#)]
56. Han, J.; Weng, X.; Bi, K. Antioxidants from a Chinese Medicinal Herb—*Lithospermum erythrorhizon*. *Food Chem.* **2008**, *106*, 2–10. [[CrossRef](#)]
57. Badawy, A.; Hassanean, H.; Ibrahim, A.K.; Habib, E.S.; El-Magd, M.A.; Ahmed, S.A. Isolates from *Thymelaea hirsuta* Inhibit Progression of Hepatocellular Carcinoma In Vitro And In Vivo. *Nat. Prod. Res.* **2021**, *35*, 1799–1807. [[CrossRef](#)] [[PubMed](#)]
58. Muhammad, A.; Tel-Çayan, G.; Öztürk, M.; Duru, M.E.; Nadeem, S.; Anis, I.; Ng, S.W.; Shah, M.R. Phytochemicals from *Dodonaea viscosa* and Their Antioxidant and Anticholinesterase Activities with Structure–Activity Relationships. *Pharm. Biol.* **2016**, *54*, 1649–1655. [[CrossRef](#)]
59. Mumtaz, A.; Mohammad, A.; Khair, Z.; Habib, A.; Nazia, A.; Itrat, A.; Shah, M.R. Antiproliferative Activity and Chemical Constituents of *Hypericum oblongifolium*. *J. Chem. Soc. Pak.* **2011**, *33*, 772–777.
60. Khan, R.; Malik, A.; Adhikari, A.; Qadir, M.I.; Choudhary, M.I. Conferols A and B, New Anti-Inflammatory 4-Hydroxyisoflavones from *Caragana conferta*. *Chem. Pharm. Bull.* **2009**, *57*, 415–417. [[CrossRef](#)]
61. Yodsauwe, O.; Karalai, C.; Ponglimanont, C.; Tewtrakul, S.; Chantrapromma, S. Potential Anti-Inflammatory Diterpenoids from the Roots of *Caesalpinia mimosoides* Lamk. *Phytochemistry* **2010**, *71*, 1756–1764. [[CrossRef](#)]
62. Ibrar, A.; Khan, I.; Abbas, N. Structurally Diversified Heterocycles and Related Privileged Scaffolds as Potential Urease Inhibitors: A Brief Overview. *Arch. Pharm.* **2013**, *346*, 423–446. [[CrossRef](#)]
63. Du, H.; Wang, Y.; Hao, X.; Li, C.; Peng, Y.; Wang, J.; Liu, H.; Zhou, L. Antimicrobial Phenolic Compounds from *Anabasis aphylla* L. *Nat. Prod. Commun.* **2009**, *4*, 385–388. [[CrossRef](#)] [[PubMed](#)]
64. Tchuenmogne, A.M.T.; Donfack, E.V.; Kongue, M.D.T.; Lenta, B.N.; Ngouela, S.; Tsamo, E.; Sidhu, N.; Dittrich, B.; Laatsch, H. Ingacamerounol, A New Flavonol and Other Chemical Constituents from Leaves and Stem Bark of *Inga edulis* Mart. *Bull. Korean Chem. Soc.* **2013**, *34*, 3859–3862. [[CrossRef](#)]
65. Wu, P.-L.; Wu, T.-S.; He, C.-X.; Su, C.-H.; Lee, K.-H. Constituents from the Stems of *Hibiscus taiwanensis*. *Chem. Pharm. Bull.* **2005**, *53*, 56–59. [[CrossRef](#)] [[PubMed](#)]
66. Daniels, D.G.H.; Martin, H.F. Antioxidants in Oats: Mono-esters of Caffeic and Ferulic Acids. *J. Sci. Food Agric.* **1967**, *18*, 589–595. [[CrossRef](#)]
67. Sonar, V.P.; Corona, A.; Distinto, S.; Maccioni, E.; Meleddu, R.; Fois, B.; Floris, C.; Malpure, N.V.; Alcaro, S.; Tramontano, E.; et al. Natural Product-Inspired Esters and Amides of Ferulic and Caffeic Acid as Dual Inhibitors of HIV-1 Reverse Transcriptase. *Eur. J. Med. Chem.* **2017**, *130*, 248–260. [[CrossRef](#)] [[PubMed](#)]
68. Vuolo, M.M.; Lima, V.S.; Junior, M.R.M. Phenolic compounds: Structure, classification, and antioxidant power. In *Bioactive Compounds*; Elsevier: Amsterdam, The Netherlands, 2019; pp. 33–50.
69. Gao, Q.; Li, Y.; Li, Y.; Zhang, Z.; Liang, Y. Antioxidant and Prooxidant Activities of Phenolic Acids Commonly Existed in Vegetables and Their Relationship with Structures. *Food Sci. Technol.* **2022**, *42*, e07622. [[CrossRef](#)]
70. Gonçalves, A.C.; Falcão, A.; Alves, G.; Silva, L.R.; Flores-Félix, J.D. Antioxidant Activity of the Main Phenolics Found in Red Fruits: An in Vitro and in Silico Study. *Food Chem.* **2024**, *452*, 139459. [[CrossRef](#)]

71. Nenadis, N.; Lazaridou, O.; Tsimidou, M.Z. Use of Reference Compounds in Antioxidant Activity Assessment. *J. Agric. Food Chem.* **2007**, *55*, 5452–5460. [[CrossRef](#)]
72. Jork, H.; Funk, W.; Fischer, W.; Wimmer, H.; Burns, D.T. *Thin-Layer Chromatography: Reagents and Detection Methods*; VCH: Weinheim, Germany, 1990.
73. Móricz, Á.M.; Ott, P.G.; Morlock, G.E. Discovered Acetylcholinesterase Inhibition and Antibacterial Activity of Polyacetylenes in Tansy Root Extract via Effect-Directed Chromatographic Fingerprints. *J. Chromatogr. A* **2018**, *1543*, 73–80. [[CrossRef](#)]
74. Schreiner, T.; Sauter, D.; Friz, M.; Heil, J.; Morlock, G.E. Is Our Natural Food Our Homeostasis? Array of a Thousand Effect-Directed Profiles of 68 Herbs and Spices. *Front. Pharmacol.* **2021**, *12*, 755941. [[CrossRef](#)] [[PubMed](#)]

Disclaimer/Publisher’s Note: The statements, opinions and data contained in all publications are solely those of the individual author(s) and contributor(s) and not of MDPI and/or the editor(s). MDPI and/or the editor(s) disclaim responsibility for any injury to people or property resulting from any ideas, methods, instructions or products referred to in the content.